Desalination and Water Treatment
www.deswater.com

doi: 10.1080/19443994.2012.750806

51 (2013) 3558–3575
April

Taylor & Francis
Taylor & Francis Group

Simultaneous removal of aluminum, iron, copper, zinc, and lead from aqueous solution using raw and chemically treated *African beech* wood sawdust

Nour T. Abdel-Ghani[a,*], Ghadir A. El-Chaghaby[b], Farag S. Helal[c]

[a]*Faculty of Science, Chemistry Department, Cairo University, Giza, Egypt*
Tel. +235676614; Fax: +235728843; email: noureta2002@yahoo.com
[b]*RCFF, Agricultural Research Center, Giza, Egypt*
[c]*Science & Technology Center of Excellence, Ministry of Military Production, Cairo, Egypt*

Received 25 May 2012; Accepted 29 October 2012

ABSTRACT

The present study investigates the use of raw and chemically modified *African beech* sawdust for the simultaneous removal of aluminum, iron, copper, zinc, and lead from aqueous solution. Batch adsorption studies were carried out at different operational conditions including: contact time, solution pH, metal ions concentrations, and adsorbents loading weights. The adsorption reached its equilibrium after a contact time of 240 min. The point of pH zero charge was found to be between 4 and 6.5 for raw and chemically treated sawdust, respectively. The spontaneous nature of the adsorption reaction was confirmed by the thermodynamic studies. The properties of the prepared adsorbents were characterized by TGA, FTIR, and SEM analysis. The kinetic and equilibrium studies suggested that the experimental data best fitted the pseudo-second-order kinetic and the Langmuir isotherm models, respectively. The recovery of the adsorbed ions was successfully achieved using different desorption solutions.

Keywords: Adsorption; *African beech*; Langmuir; Pseudo-second-order kinetic; Desorption

1. Introduction

Water pollution is a global environmental problem. For a long time, industrial wastes containing heavy metals have been released into the environment. These metals contaminate surface water, groundwater, seawater, soil, and bottom sediments and often accumulate in plants and animals, which are consumed by humans [1]. Metal ions can be released into environment by means of various industrial processes such as mining, metallurgical engineering, battery manufacturing, nuclear power operations, chemical manufacturing, pharmaceuticals, galvanizing, paints, pigments, insecticides, and cosmetics [2].

Heavy metal ions are stable and persistent in the environment since they cannot be degraded and destroyed. These metal ions can be harmful to many living organisms once spread through food chain. Aluminum, iron, copper, zinc, and lead are important constituents of some industrial wastewaters including battery recycling, electroplating, metal finishing, painting, etc. These constituents are toxic in varying degrees to micro-organisms and their pres-

---

*Corresponding author.

ence in excessive quantities will interfere with many beneficial uses of the water because of their toxicity. Therefore, they must be taken into consideration in the design of a biological treatment plant. Exposure to heavy metal contamination has been found to cause kidney damage, liver damage, and anemia in low doses, and in high concentrations, heavy metals can be carcinogenic [3].

The conventional methods for heavy metal removal from wastewater include precipitation, ion exchange, adsorption, evaporation, redox, membrane process, extraction, biological, and chemical processes [4]. Among these, the adsorption, with the selection of suitable adsorbents, can be an effective technique for the removal of heavy metals from wastewater [5].

The use of natural materials for heavy metals removal by adsorption as a cost-effective method for water treatment is of growing research interest. Natural materials that are available in large quantities or certain waste from agricultural and manufacture operations may have potential to be used as low-cost adsorbents, as they represent unused resources, widely available and are environment friendly [6]. Many researchers have investigated the use of various natural agricultural waste materials as biosorbents for the removal of metal ions from water bodies. These agricultural-based biosorbents included maize leaf [7], olive pomace [8], coconut and seed hulls of the palm tree [9], rice husks, maize cobs and sawdust [10], *Typha domingensis* leaf powder [11], date seeds [12], and lotus-stalks [13].

Large quantities of sawdust are produced as a waste of furniture industry which is one of the traditional Egyptian industries. The industry is highly dependent on imported wood for raw materials especially *African beech* trees wood. Sawdust has little or no economic value, and it is disposed in large amounts during the years [14]. Thus, aim of the present study was to assess the ability of *African beech* sawdust (raw and chemically treated) to simultaneously remove aluminum, iron, copper, lead, and zinc ions from their mixed aqueous solutions under different operational conditions.

2. Experimental

2.1. Adsorbents preparation

Sawdust was collected from Egyptian furniture factories. The sawdust was washed several times with deionized water to remove surface impurities, and then it was oven dried at 105˚C for 24 h. The dried biomass was stored in a desiccator for further use. This was used as the first adsorbent (raw sawdust). The second adsorbent (chemically treated sawdust) was prepared following the procedure described by Kalavathy and Miranda [15] with some modification. The dried saw dust was mixed with sodium hydroxide at impregnation ratio of 1:4. The mixture was kept at 24 h so that the reagent was fully adsorbed onto the raw material. The saw dust was filtered and washed with distilled water until the filtrate reached constant pH. The samples were then dried at 110˚C until they reached a constant weight.

2.2. Adsorbents characterization

The two prepared adsorbents (raw and chemically treated sawdust) were characterized by FTIR and SEM analyses using Nicolet, AVATAR FTIR-370 Csl and Quanta 250-FEI scanning electron microscope, respectively. Thermogravimetric analysis of the adsorbents was also carried out using a thermogravimetric analyser (TGA-Q 500).

2.3. Adsorbate solutions

The stock solutions (1000 mg/L) of metal ions (aluminum, iron, copper, zinc, and lead) were prepared by dissolving their corresponding nitrate salts in deionized water. During the experiment, the solutions were further diluted to the required concentrations before use. All the chemicals used were of analytical reagent grade and were obtained from Fluka.

2.4. Adsorption studies

Batch adsorption studies were carried out at room temperature. The effect of contact time on simultaneous metal ions removal was investigated by mixing 50 mL mixed metal ions solution with 0.5 g of sawdust in conical flasks for different time intervals. The solution–adsorbent mixtures were stirred at 100 rpm in a shaking water bath and at the end of predetermined time interval the suspensions were separated by filtration. The solutions were analyzed for their metal ion concentrations using an atomic absorption spectrometer, AAS (Shimadzu AA-6300) at the following wavelengths: Al (396.153 nm), Fe (259.939 nm), Cu (324.752 nm), Zn (213.857 nm), and Pb (220.353 nm).

The effect of metal ions concentration on their removal was studied at the pre-determined equilibrium time.

Metal ions removal percentages were determined using Eq. (1)

$$\text{Removal}\,\% = (C_i - C_f) \times 100/C_i \tag{1}$$

where C_i and C_f are the initial and final concentrations of metal ions (mg/L) in the solution

Adsorption capacity was calculated using Eq. (2)

$$Q = (C_i - C_f) \times V/W \tag{2}$$

where Q is the adsorption capacity (mg/g), C_i is the initial concentration of metal in solution (mg/L), C_f is the equilibrium concentration of metal in solution (mg/L), V is the volume of metal ion solution (L), and W is the weight of the adsorbent (g).

2.5. Kinetics study

The pseudo-first-order model [16], the pseudo second-order model [17], and the intra-particle diffusion model [18] were investigated to describe the adsorption kinetics of the studied metal ions onto the adsorbents prepared from *African beach* sawdust. The equations describing the three tested kinetic models are summarized in Table 1.

2.6. Equilibrium modeling

The experimental data were analyzed using the Langmuir [19], Freundlich [20], and Temkin [21] isothermal models. The equations describing the three tested equilibrium models are summarized in Table 2.

2.7. Desorption study

For the desorption study, 0.5 g sawdust was contacted with 50 mL mixed ions solution (25 mg/L). After adsorption experiment, the biomass was removed by filtration and washed with distilled water for three times, to remove residual ions on the surface. Then it was transferred to 50 mL desorbent solutions: 0.1 M HCl, HNO_3, and H_2SO_4 and 0.5 M NaOH. The mixtures were shaken for 24 h, then the filtrates were analyzed to determine the concentration of ions after desorption.

The recovery percentage was calculated following Eq. (3):

$$\text{Recovery}\ \% = (C_d/C_a) \times 100 \tag{3}$$

where C_d is the amount of metal ions desorbed at equilibrium in mg/g and C_a is the metal uptake at equilibrium in mg/g, for each cycle.

3. Results and discussion

3.1. Effect of contact time

The effect of contact time on the simultaneous removal of aluminum, iron, copper, zinc, and lead from their mixed ions solution using raw and chemically treated sawdust is given in Fig. 1.

It was observed that the removal of metal ions was initially rapid which could be attributed to the

Table 1
Kinetic models linear form equations

Kinetic model	Linear equation form		Terms definitions
Pseudo-first-order	$\ln(Q_e - Q_t) = \ln Q_e - k_1 t$	(3)	Q_e: equilibrium capacity in mg/g Q_t: capacity at time (t) in mg/g
Pseudo-second-order	$t/Q_t = (1/k_2 Q_e^2) + t/Q_e$	(4)	t: time in minutes K_1: rate constant of first-order adsorption (min^{-1})
Intraparticle diffusion	$Q_t = k_p \sqrt{t} + C$	(5)	K_2: rate constant of second-order adsorption ($g\,mg^{-1}\,min^{-1}$) K_p: intraparticle diffusion rate constant ($mg\,g^{-1}\,min^{-1/2}$) C: intercept of intraparticle diffusion ($mg\,g^{-1}$)

Table 2
Equilibrium models linear form equations

Isothermal model	Linear equation form		Terms definition
Langmuir	$C_{eq}/Q_e = 1/bQ_{max} + C_{eq}/Q_{max}$	(6)	C_{eq}: equilibrium concentration in mg/L Q_e: equilibrium capacity in mg/g
Freundlich	$\log Q_e = \log K_f + (1/n)\log C_{eq}$	(7)	Q_{max}: maximum capacity in mg/g b (L/mg) is Langmuir constant
Temkin	$Q_{eq} = a_t + b_t \ln C_{eq}$	(8)	K_f and n are Freundlich constants b_t and a_t are Temkin isotherm constants

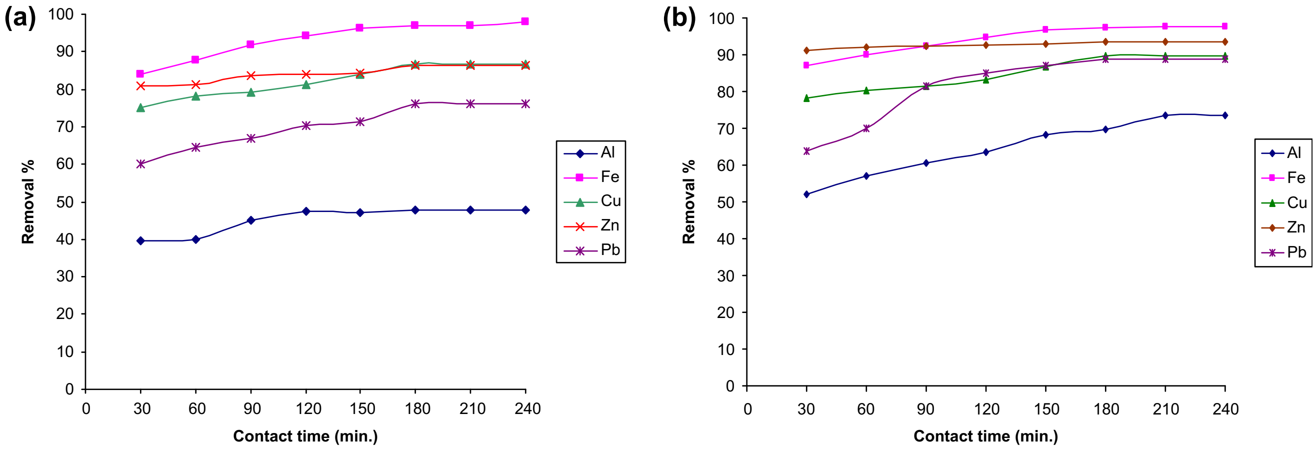

Fig. 1. Effect of contact time on the simultaneous removal of Al(III), Fe(III), Cu(II), Zn(II), and Pb(II) from their mixed ions solution by adsorption onto (a) untreated sawdust, (b) chemically treated sawdust; initial ions concentration in the mixed ions solution: 25 mg/L; pH: initial mixed ions solution pH; biomass weight: 0.5 g/50 mL; shaking speed: 100 rpm; temp.: 25°C.

availability of larger surface area of the sawdust for the adsorption of these ions [22]. The adsorption rate then slowed down with increasing contact time until reaching equilibrium. This is due to the fact that as the surface adsorption sites became exhausted, the rate of uptake is controlled by the rate of transport from the exterior to the interior sites of the adsorbent particles [22].

From Fig. 1 it can be seen that the adsorption of aluminum ions reached its maximum after 120 and 210 min on raw and treated sawdust, respectively. Whereas the maximum adsorption for iron, copper, zinc, and lead ions was attained after 180 min of contact on both adsorbents used. Based on these results all further experiments were performed at 240 min to ensure equilibrium for all studied ions.

Comparing the metal ions removal percentages obtained at equilibrium, it was observed that under the same experimental conditions chemical treatment of sawdust caused an enhancement in the removal percentages compared to untreated sawdust. Treating the sawdust with NaOH causes an increase in the adsorbent surface negative charge which in turns increases the surface ability to attract positively charged ions. It has been reported that the treatment with sodium hydroxide solution increases adsorption capacities of modified sawdusts in removing different metal ions from aqueous solutions [15,23].

According to Rehman et al. [24], treating sawdust with sodium hydroxide solution leads to an increase in the adsorption property of the adsorbent. Carboxylate ligands are believed to be responsible for metal binding by the biomasses. This means that metal binding can be enhanced by increasing the number of carboxylate ligands in the biomass. Cellulose, hemicellulose, and lignin, which are major constituents of sawdust, contain methyl esters, which do not bind metal ions significantly. However, these methyl esters can be modified to carboxylate ligands by treating the biomass with a base such as sodium hydroxide, thereby increasing the metal-binding ability of the biomass. The NaOH treatment of the biomass leads to the removal of lignin allowing more of the cellulose and hemicellulose [25].

3.2. Adsorption kinetic studies

Mathematical models that can describe the behavior of a batch sorption process operated under different experimental conditions are very useful for scale-up studies or process optimization [26]. Three kinetic models were used in this study including the pseudo-first-order, pseudo-second-order and intraparticle diffusion equations developed by Lagergren [16], Ho and McKay [17], and Weber and Morris [18], respectively. The experimental Q_e values were compared to those obtained from the tested models. The plots representing the three studied kinetic models are shown in Figs. 2–4. The three kinetic models' constants along with their regression coefficients data for aluminum, iron, copper, zinc, and lead removal using raw and chemically treated sawdust are given in Tables 3 and 4, respectively. The best model fitting the experimental data was selected based on both determination coefficient (R^2) and the calculated Q_e values.

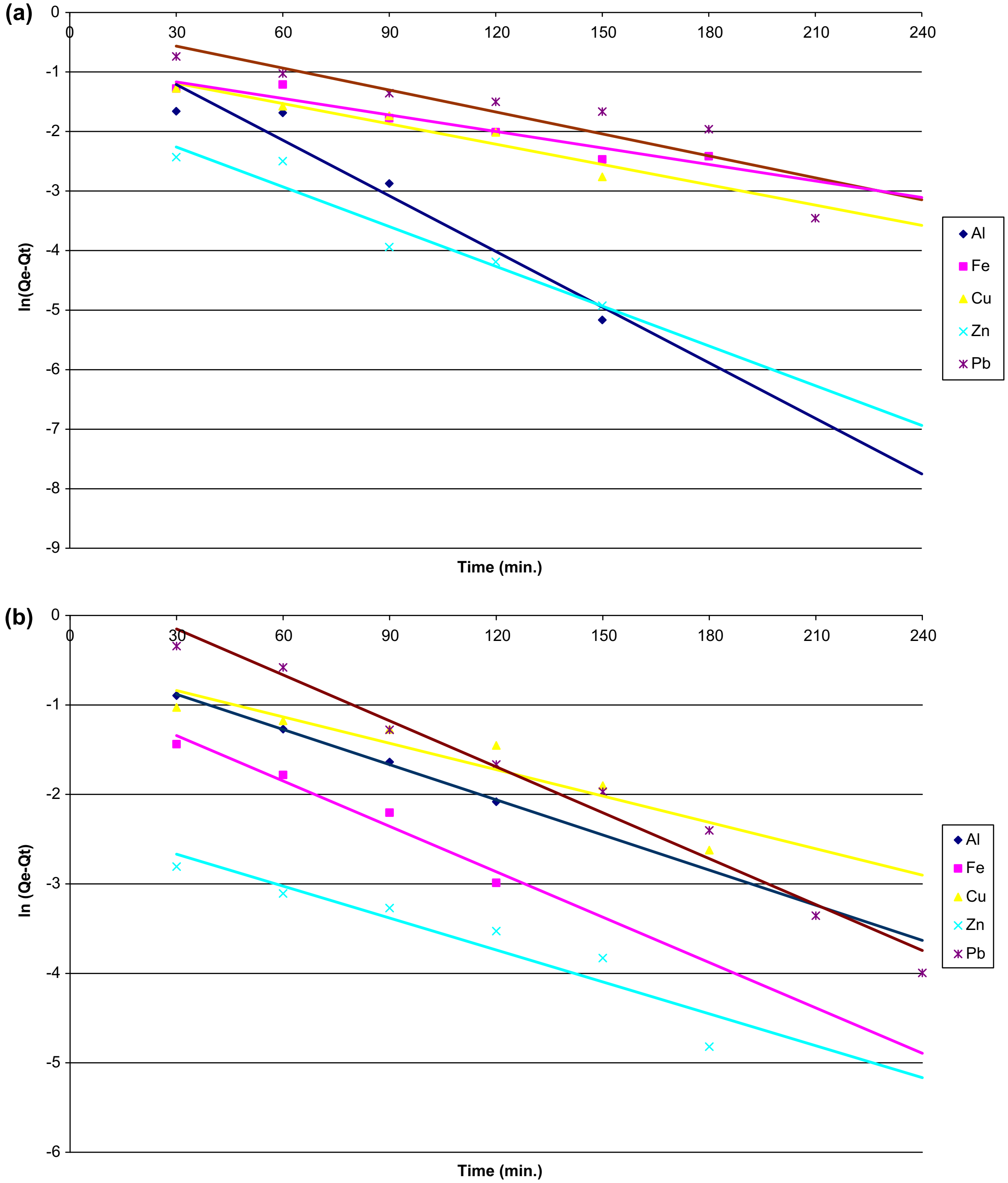

Fig. 2. Pseudo-first-order kinetic plots for the simultaneous removal of Al(III), Fe(III), Cu(II), Zn(II), and Pb(II) from their mixed ions solution by adsorption onto (a) untreated sawdust, (b) chemically treated sawdust; initial ions concentration in the mixed ions solution: 25 mg/L; pH: initial mixed ions solution pH; biomass weight: 0.5 g/50 mL; shaking speed:100 rpm; temp.: 25˚C.

3.2.1. Lagergren pseudo-first-order kinetic model

A plot of log (Q_e–Q_t) vs. t gives a linear trace from which the values of K_1 and Q_e can be determined from the slope and intercept. As can be seen from Tables 3 and 4, the obtained R^2 values for the pseudo-first-order model for the two studied adsorbents were relatively high however close inspection of the model fit and experimental observations in Figs. 2 and 3 suggest that the application of this model is inappro-

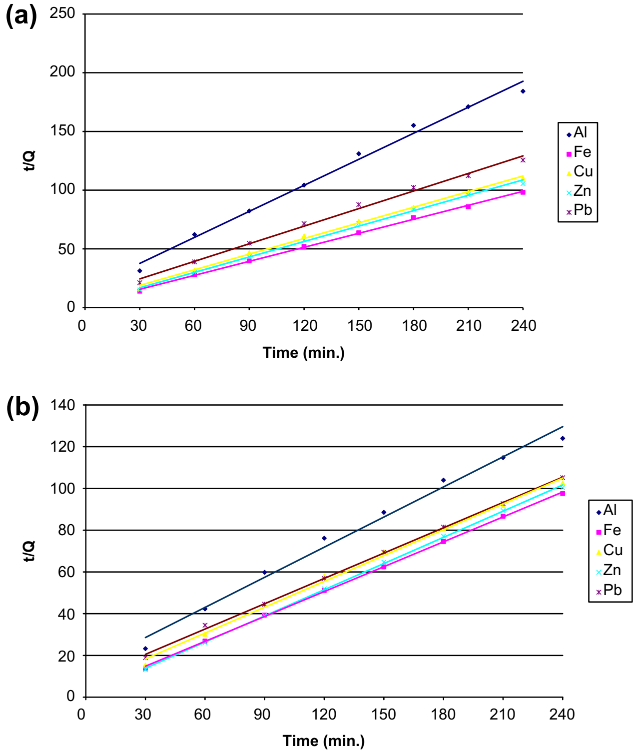

Fig. 3. Pseudo-second-order kinetic plots for the simultaneous removal of Al(III), Fe(III), Cu(II), Zn(II), and Pb(II) from their mixed ions solution by adsorption onto (a) untreated sawdust, (b) chemically treated sawdust; initial ions concentration in the mixed ions solution: 25 mg/L; pH: initial mixed ions solution pH; biomass weight: 0.5 g/50 mL; shaking speed:100 rpm; temp.: 25°C.

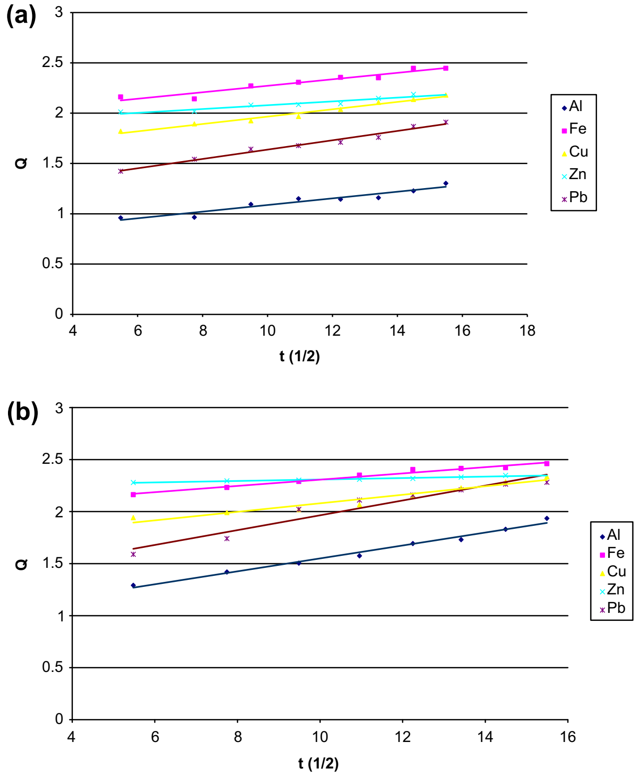

Fig. 4. Intraparticle diffusion mechanism plots for the simultaneous removal of Al(III), Fe(III), Cu(II), Zn(II), and Pb(II) from their mixed ions solution by adsorption onto (a) untreated sawdust, (b) chemically treated sawdust; initial ions concentration in the mixed ions solution: 25 mg/L; pH: initial mixed ions solution pH; biomass weight: 0.5 g/50 mL; shaking speed:100 rpm; temp.: 25°C.

priate as experimental observations are non-linear when plotted in this manner. Also it can be noticed that there is no agreement between experimentally observed equilibrium adsorption and those derived using the pseudo-first-order model. This suggests that the adsorption of the studied ions onto both suggested adsorbents did not follow pseudo-first-order kinetics.

3.2.2. Pseudo-second-order kinetics model

Pseudo-second-order adsorption parameters $Q_{e,\mathrm{cal}}$ and $K_{2,\mathrm{ad}}$ were obtained by plotting (t/Q_t) vs. (t). The pseudo-second-order model fitted the experimental data with high determination coefficient values ($R^2 > 0.99$) for all the studied metal ions onto both adsorbents (Tables 3 and 4).

The values of the equilibrium capacity ($Q_{\mathrm{eq.}}$) calculated from the pseudo-second order model were found to be very close to the experimental equilibrium capacity values. The results suggest the applicability of the pseudo-second-order model. The obtained values of ($K_{2,\mathrm{ad}}$) of different metal ions lead to the conclusion that the reaction taking place is pseudo-second order suggesting chemical sorption between the adsorbate and adsorbent [15]. The values of ($K_{2,\mathrm{ad}}$) also indicated that metal ions are preferentially adsorbed onto raw sawdust in the following order [Zn(II) > Al(III) > Cu(II) > Fe(III) > Pb(II)], whereas the adsorption rate onto chemically treated sawdust was in the order [Zn(II) > Cu(II) > Al(III) > Fe(III) > Pb(II)].

3.2.3. Intraparticle diffusion mechanism

The overall rate of adsorption can be described by the following three steps [27]: (1) film or surface diffusion where the sorbate is transported from the bulk solution to the external surface of sorbent, (2) intraparticle or pore diffusion, where sorbate molecules move into the interior of sorbent particles, and (3) adsorption on the interior sites of the sorbent. Boparai et al. [28] suggested that since the adsorption step is very

Table 3
The first-order, second-order and intraparticle diffusion models rate constants for Al^{3+}, Fe^{3+}, Zn^{2+}, Cu^{2+}, and Pb^{2+} adsorption using raw sawdust

	First-order kinetic model			Pseudo-second-order model			Intraparticle diffusion model			Q_e Experimental (mg/g)
	$K_{1,ad}$ (min^{-1})	$Q_{eq.}$ (mg/g)	R^2	$K_{2,ad}$ (g/mg.min)	$Q_{eq.}$ (mg/g)	R^2	K_p ($mg/g.min^{1/2}$)	C (mg/g)	R^2	
Al^{3+}	0.031	0.758	0.938	0.035	1.35	0.991	0.033	0.756	0.924	1.200
Fe^{3+}	0.009	0.392	0.925	0.027	2.52	0.998	0.032	1.951	0.927	2.400
Cu^{2+}	0.011	0.427	0.913	0.029	2.25	0.997	0.034	1.621	0.958	2.100
Zn^{2+}	0.022	0.203	0.929	0.040	2.29	0.996	0.019	1.890	0.901	2.200
Pb^{2+}	0.012	0.821	0.813	0.026	2.00	0.994	0.046	1.174	0.977	1.900

Temperature: 25℃; agitation rate: 100 rpm; biomass concentration: 0.5 g/50 mL; pH: 2.5; initial mixed ions concentrations: 25 mg/L.

Table 4
The first-order, second-order and intraparticle diffusion models rate constants for Al^{3+}, Fe^{3+}, Zn^{2+}, Cu^{2+} and Pb^{2+} adsorption using treated sawdust

	First-order kinetic model			Pseudo-second-order model			Intraparticle diffusion model			Q_e experimental
	$K_{1,ad}$ (min^{-1})	$Q_{eq.}$ (mg/g)	R^2	$K_{2,ad}$ (g/mg.min)	$Q_{eq.}$ (mg/g)	R^2	K_p ($mg/g.min^{1/2}$)	C (mg/g)	R^2	
Al^{3+}	0.013	0.613	0.998	0.015	2.078	0.990	0.062	0.929	0.985	1.900
Fe^{3+}	0.017	0.433	0.961	0.034	2.515	0.999	0.030	2.006	0.977	2.400
Cu^{2+}	0.010	0.580	0.862	0.019	2.427	0.995	0.041	1.671	0.941	2.200
Zn^{2+}	0.012	0.099	0.885	0.096	2.391	0.999	0.007	2.238	0.952	2.400
Pb^{2+}	0.017	1.436	0.975	0.013	2.481	0.998	0.071	1.252	0.936	2.300

Temperature: 25℃; agitation rate: 100 rpm; biomass concentration: 0.5 g/50 mL; pH: 2.5; initial mixed ions concentrations: 25 mg/L.

rapid, it is assumed that it does not influence the overall kinetics. The overall rate of adsorption process, therefore, will be controlled by either surface diffusion or intraparticle diffusion. The Weber–Morris intraparticle diffusion model has often been used to determine if intraparticle diffusion is the rate-limiting step [28]. The intraparticle diffusion mechanism suggests proportionality between the adsoption capacity and the square root of the time. The plots of the amount of ions adsorbed against the square root of the time (Figs. 2 and 3) were used to determine the rate constants (K_p) and the intercept (C) for intraparticle diffusion mechanism of different metal ions. The plots are straight lines for both the adsorbents but not passing through the origin, indicating that intra-particle diffusion is not the only rate-limiting factor for the adsorption of the studied metal ions. The deviation of the plots linearity from the origin could be attributed to the variation of mass transfer in the initial and final stages of adsorption [29].

As seen from Tables 3 and 4, the obtained K_p values led to the conclusion that the intraparticle diffusion also contributes to the rate determining step. The values of the intercept (C) provide information related to the thickness of the boundary layer [30]. Larger intercepts suggest that surface diffusion has a larger role as the rate-limiting step. The intraparticle diffusion model was found to be applicable to the obtained experimental data. Thus according to Gupta et al. [31] besides for the adsorption on the outer surface of adsorbent, there is also possibility of transport of adsorbent ions from the solution to the pores of the adsorbent due to stirring on batch process.

3.3. Equilibrium modeling

Equilibrium isotherm models are of great importance in designing an efficient adsorption system. These models provide information on the capacity of the adsorbent or the amount required to remove a unit mass of pollutant under the system conditions [32]. The equation parameters of these equilibrium models often provide some insight into the adsorption mechanism, the surface properties of an adsorbent, and affinity of the adsorbent for an adsorbate [33].

To evaluate the adsorption capacity of raw and chemically treated African beech sawdust for the removal of Al(III), Fe(III), Cu(II), Zn(II), and Pb(II) ions from their mixed ions solution, the Langmuir, Freundlich and Temkin isotherm models were used. Figs. 5–7, illustrate the three isotherm results obtained after 240 min. of contact time, initial ion solution pH, adsorbent dose of 0.5 g/50 mL, a temperature of 25℃ and at different initial ions concentrations (5-100 mg/L).

Langmuir's isotherm model suggests that the uptake occurs on homogeneous surface by monolayer sorption without interaction between adsorbed ions. The linear form of Langmuir isotherm equation is represented by Eq. (6) in Table 2. According to the model's equation, a plot of C_{eq}/Q_e vs. C_{eq} (Fig. 5) should be a straight line with a slope $(1/b)$ and an intercept as $1/Q_{\max}$.

Plots of C_{eq}/Q_e against C_{eq} were obtained and the model's determination coefficient values and the constants $Q_{\max}$ and b were calculated and reported in Table 5.

As seen from Table 5, high determination coefficient values ($R^2 = 0.92$–0.99) were obtained for the Langumuir model indicating a good agreement between the experimental parameters and confirming the monolayer adsorption of Al(III), Fe(III), Cu(II), Zn(II), and Pb(II) ions onto both studied adsorbents surfaces.

The Freundlich and Temkin models were also tried to fit the obtained experimental data and the two models constants as well as their determination coefficients are given in Table 5.

Freundlich expression is an empirical equation based on sorption on a heterogeneous surface [20]. The empirical Freundlich equation based on sorption on a heterogeneous surface is given as Eq. (7) in Table 2. The Freundlich constants (K_f) and (n) are characteristic of the system and are indicators of adsorption capacity and adsorption intensity [11].

The derivation of the Temkin isotherm [21] assumes that the fall in the heat of sorption is linear rather than logarithmic, as implied in the Freundlich equation. The Temkin isotherm is generally applied in the form given by Eq. (8), Table 2. Temkin's constants b_{t} and a_{t} are related to the adsorption capacity of the adsorbent.

As can be seen from Table 5, the Freundlich and Temkin isotherm models did not fit well the experimental data. Both models showed determination coefficient values lower than those obtained for the Langmuir model. The fact that the Langmuir isotherm fits the experimental data may be also attributed to homogeneous distribution of active sites onto adsorbent surface, since the Langmuir equation assumes that the surface is homogeneous [34].

The Standard Gibb's free energy change ΔG° is the fundamental criterion of spontaneity. Reactions occur spontaneously at a given temperature if ΔG° is a negative value. The very useful relationship between standard free energy change, ΔG°, and the Langmuir constant, b, is given by Singh et al. [35] as $\Delta G^\circ = -RT \ln b$.

where R is universal gas constant (8.314 J/mol K), and T is the absolute temperature in K.

An estimation of the values of ΔG° for the adsorption process of Al(III), Fe(III), Cu(II), Zn(II), and Pb(II) were calculated and they are listed in Table 6. The negative values of ΔG° confirm the feasibility of the process and the spontaneous nature of sorption [36].

In order to evaluate the applicability of using *African beech* sawdust in the simultaneous removal of Al (III), Fe(III), Cu(II), Zn(II), and Pb(II), our experimental data of values $Q_{\max}$ were compared with $Q_{\max}$ obtained with other adsorbents cited in the literature (Table 7). It can be seen from this table that our results are comparable to or some what better than previously reported results noting that we worked on mixed metal ions solution whereas previous studies involved single ion removal.

3.4. Adsorbents characterization

3.4.1. Determination of (pH pzc)

Determination of pH point of zero charge is of fundamental importance in environmental science [15]. It determines how easily a substrate is able to adsorb potentially harmful ions. The pH point of zero charge (pHpzc) was carried out by taking 50 mL of 0.1 M NaCl solutions in different closed Erlenmeyer flasks. The pH of the solution ($\mathrm{pH_o}$) in each flask was adjusted to values of 2, 4, 6, 8, 10, and 12 by adding 0.1 M HCl or 0.1 M NaOH solutions. Then 0.2 g of each of the adsorbents was added and agitated in a shaker for 1 h and allowed to stay for 48 h to reach equilibrium with intermittent manual shaking. Then the final pH value ($\mathrm{pH_f}$) of the supernatant liquid was noted. The difference between the initial and final pH values ($\Delta\mathrm{pH} = \mathrm{pH_o} - \mathrm{pH_f}$) was plotted against the $\mathrm{pH_o}$. The point of intersection of the resulting curve at which $\Delta\mathrm{pH} = 0$ gave the pHpzc [40,41].

Fig. 8 shows the plot of point of zero charge (pHpzc) for the two studied adsorbents (raw and treated sawdust). According to Kalavathy and Miranda [15], the pHpzc is a point at which the surface acidic (or basic) functional groups no longer contribute to the pH value of the solution. The pHpzc of raw and chemically treated sawdust were found to be 4 and 6.5, respectively. It can be concluded that the modification of sawdust with sodium hydroxide increased its surface pH value. This is due to its increased negative charge contribution to the adsorbent surface

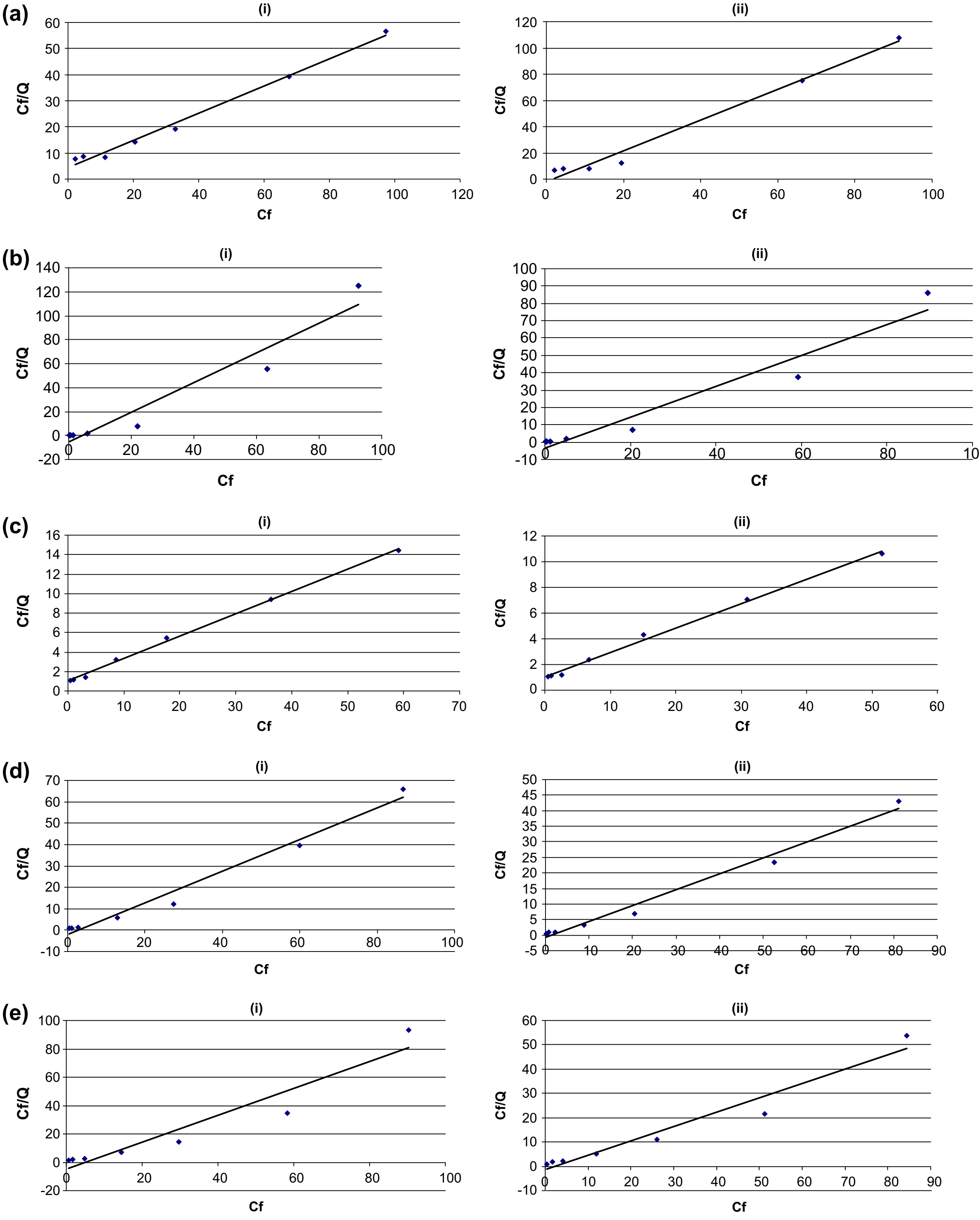

Fig. 5. (a) Langmuir isotherm for the adsorption of Al onto (i) raw and (ii) chemically treated sawdust. (b) Langmuir isotherm for the adsorption of Fe onto (i) raw and (ii) chemically treated sawdust. (c) Langmuir isotherm for the adsorption of Cu onto (i) raw and (ii) chemically treated sawdust. (d) Langmuir isotherm for the adsorption of Zn onto (i) raw and (ii) chemically treated sawdust. (e) Langmuir isotherm for the adsorption of Pb onto (i) raw and (ii) chemically treated sawdust.

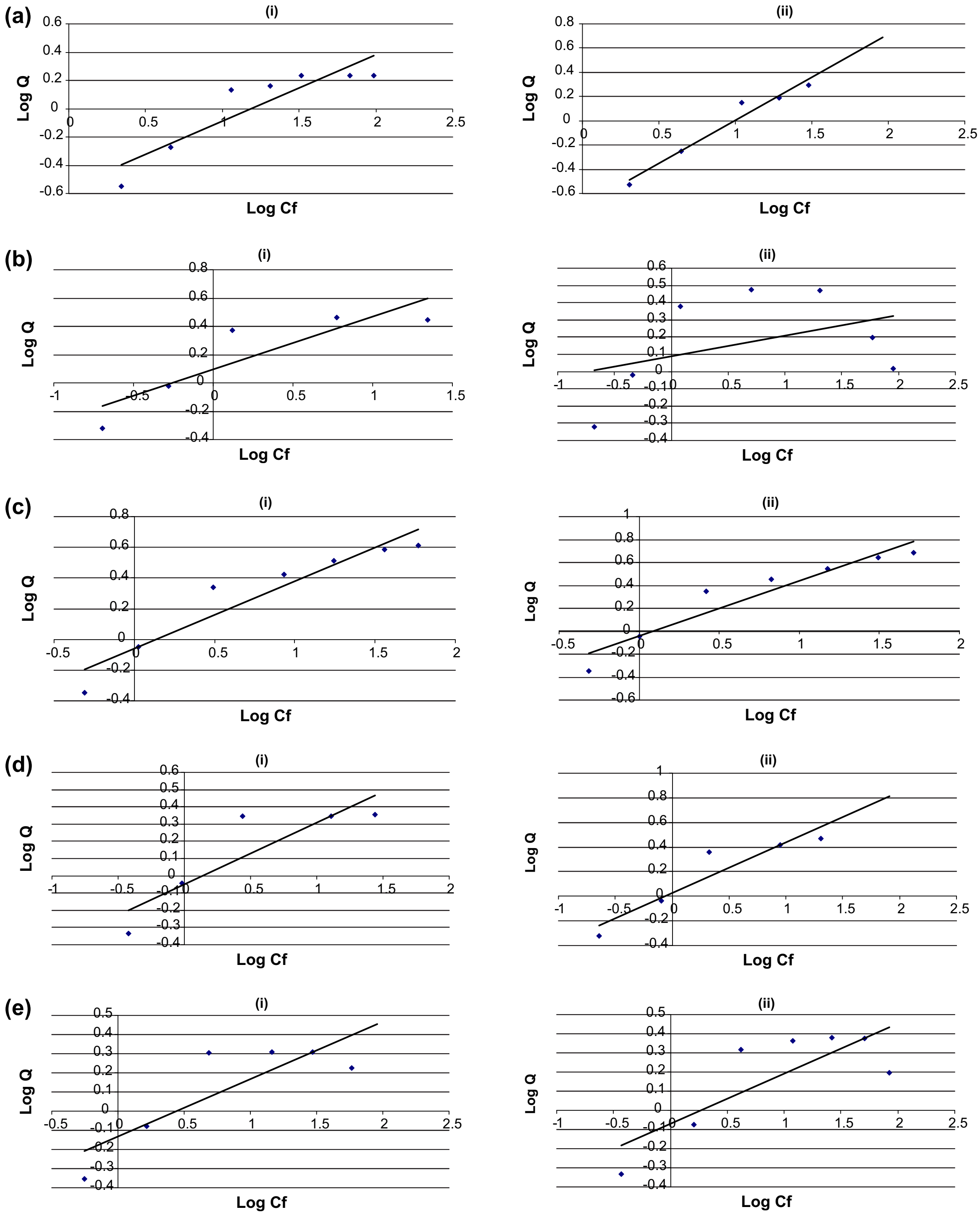

Fig. 6. (a) Freundlich isotherm for the adsorption of Al onto (i) raw and (ii) chemically treated sawdust. (b) Freundlich isotherm for the adsorption of Fe onto (i) raw and (ii) chemically treated sawdust. (c) Freundlich isotherm for the adsorption of Cu onto (i) raw and (ii) chemically treated sawdust. (d) Freundlich isotherm for the adsorption of Zn onto (i) raw and (ii) chemically treated sawdust. (e) Freundlich isotherm for the adsorption of Pb onto (i) raw and (ii) chemically treated sawdust.

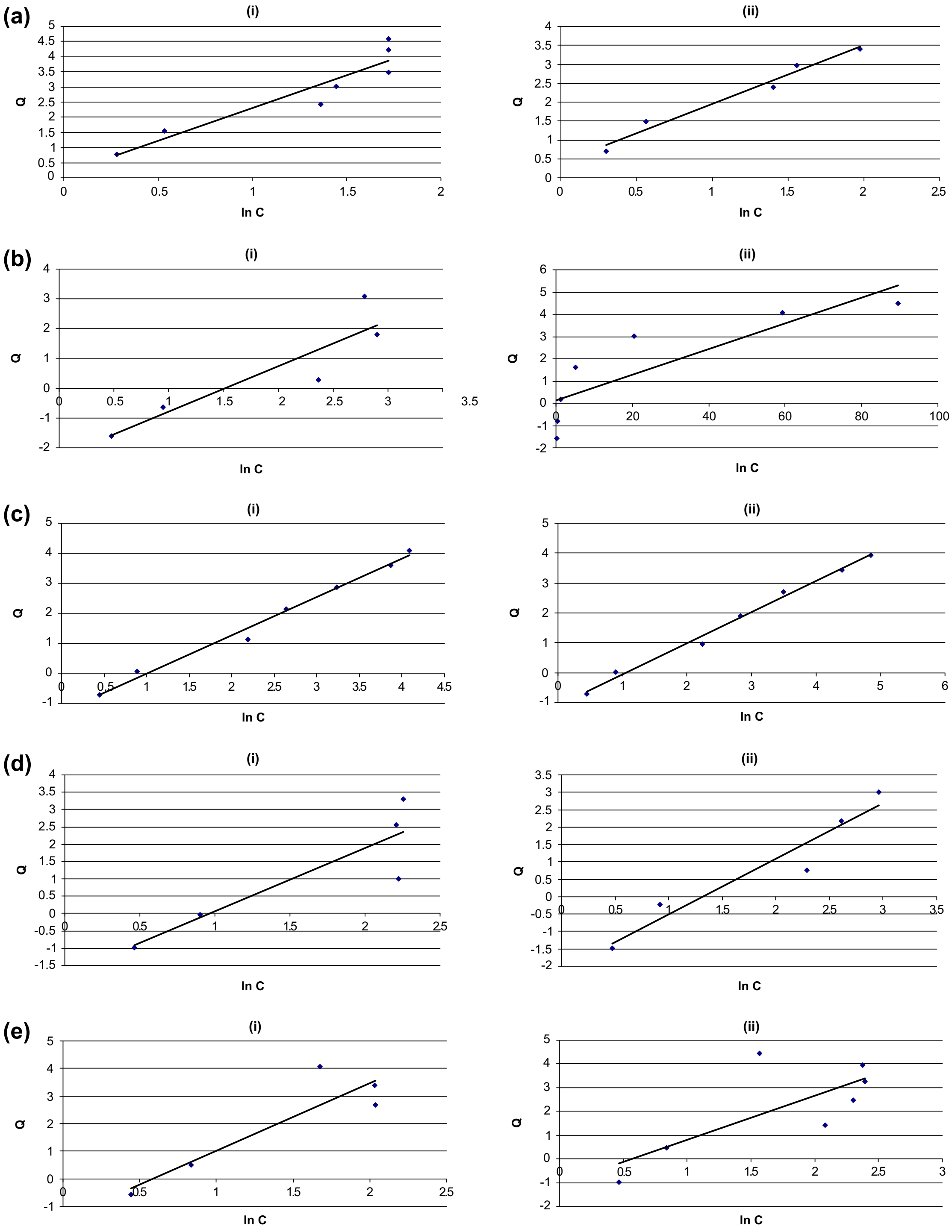

Fig. 7. (a) Temkin isotherm for the adsorption of Al onto (i) raw and (ii) chemically treated sawdust. (b) Temkin isotherm for the adsorption of Fe onto (i) raw and (ii) chemically treated sawdust. (c) Temkin isotherm for the adsorption of Cu onto (i) raw and (ii) chemically treated sawdust. (d) Temkin isotherm for the adsorption of Zn onto (i) raw and (ii) chemically treated sawdust. (e) Temkin isotherm for the adsorption of Pb onto (i) raw and (ii) chemically treated sawdust.

Table 5
Sorption isotherm coefficients of Langmuir, Freundlich, and Temkin models applied to Al^{3+}, Fe^{3+}, Cu^{2+}, Zn^{2+}, and Pb^{2+} adsorption by raw and chemically treated *African beech* sawdust

M^+	Raw *African beech* sawdust									Chemically treated *African beech* sawdust								
	Langmuir			Freundlich			Temkin			Langmuir			Freundlich			Temkin		
	$Q_{max.}$ (mg/g)	b (L/mg)	R^2	K_f	n	R^2	a_t	b_t	R^2	$Q_{max.}$ (mg/g)	b (L/mg)	R^2	K_f	n	R^2	a_t	b_t	R^2
Al^{3+}	1.914	1.208	0.990	0.571	2.123	0.822	0.148	2.163	0.884	0.854	0.733	0.984	0.493	1.403	0.965	0.405	1.542	0.973
Fe^{3+}	0.804	0.219	0.938	1.098	2.681	0.938	2.324	1.532	0.821	1.122	0.267	0.948	1.094	8.417	0.173	0.123	0.057	0.734
Cu^{2+}	4.357	0.221	0.997	0.940	2.283	0.903	1.281	1.274	0.988	5.249	0.188	0.995	0.960	2.074	0.910	1.111	1.045	0.992
Zn^{2+}	1.354	0.355	0.980	0.995	2.805	0.773	1.768	1.825	0.787	1.955	0.598	0.985	1.027	2.434	0.882	2.103	1.594	0.925
Pb^{2+}	1.059	0.198	0.918	0.875	3.343	0.704	1.452	2.463	0.821	1.689	0.406	0.953	0.932	3.813	0.645	1.038	1.855	0.560

Temperature: 25°C; agitation rate: 100 rpm; adsorbent concentration: 0.5 g/50 mL; pH: initial ions solution pH.

Table 6
Standard Gibb's free energy change ΔG° for the adsorption process of Al^{3+}, Fe^{3+}, Cu^{2+}, Zn^{2+}, and Pb^{2+} by raw and chemically treated *African beech* sawdust at 25°C

Metal ion	ΔG° (kJ/mol) (for adsorption on raw sawdust)	ΔG° (kJ/mol) (for adsorption on chemically treated sawdust)
Al^{3+}	−25.748	−24.509
Fe^{3+}	−23.321	−23.816
Cu^{2+}	−23.665	−23.264
Zn^{2+}	−24.906	−26.201
Pb^{2+}	−26.329	−28.098

[15]. NaOH also hydrolyzes lignin which is present in sawdust as binding constituent of its fibrous structure, it exposes more adsorption sites.

3.4.2. FTIR analysis

The determination of the adsorbent's surface functional groups by FTIR analysis have been widely reported [42,11,22,43]. The FTIR spectra of raw and chemically treated *African beech* sawdust before and after adsorption are given in Fig. 9. Analyzing the FTIR of raw *African beech* wood sawdust, it can be noticed that the region corresponding to high wave numbers shows a broad band centered around 3400 cm^{-1} which can be assigned to –OH stretching vibration of the surface hydroxyl groups and adsorbed water. The band at 2924 cm^{-1} could be assigned to symmetric vibration of CH_2 especially alkenes. The band at 1631 cm^{-1} could be attributed to the presence of COO, C=O groups and can also indicate the bending vibration of adsorbed water. The band at 1269 cm^{-1} can be assigned to carboxylic acids vibration and/or the C–O stretching of phenolic groups. The band at 1059 cm^{-1} is stretching vibration of C–O–C and O–H of polysaccharides. The band at around 1428 cm^{-1} could be assigned to symmetric COO-stretching motions and to the bending vibrations of aliphatic groups. FTIR spectrums showed that sawdust is mainly composed of polymeric OH groups, CH_2 and COO groups, and OH groups of polysaccharides [42].

The changes in the surface functional groups of sawdust after treatment with sodium hydroxide were also confirmed by FTIR spectra. As seen from Fig. 9 and Table 8, it was observed that there were shifts in the wave number of some peaks associated with the treatment of sawdust with sodium hydroxide. The sharp peak observed at 2924 cm^{-1} in case of raw saw-

Table 7
Maximum adsorption capacities obtained using different adsorbents previously reported in literature

Adsorbents	Q max (mg/g)					Reference
	Al^{3+}	Fe^{3+}	Cu^{2+}	Zn^{2+}	Pb^{2+}	
Raw *African beech* sawdust	1.913	0.804	4.357	1.354	1.058	Present work
Chemically treated *African beech* sawdust	0.854	1.122	5.249	1.955	1.689	Present work
Modified oak sawdust	–	–	3.220	–	–	Argun et al. [37]
Linden sawdust	–	0.350	1.900	1.425	–	Boõzić et al. [38]
Unmodified *Hevea Brasiliensis* saw dust	–	–	3.452	–	–	Kalavathy and Miranda [15]
Maple sawdust	–	–	1.790	–	3.190	Yu et al. [39]
Poplar sawdust	–	–	2.540	–	–	Sciban and Klasnja [23]
Fir sawdust	–	–	2.350	–	–	Sciban and Klasnja [23]

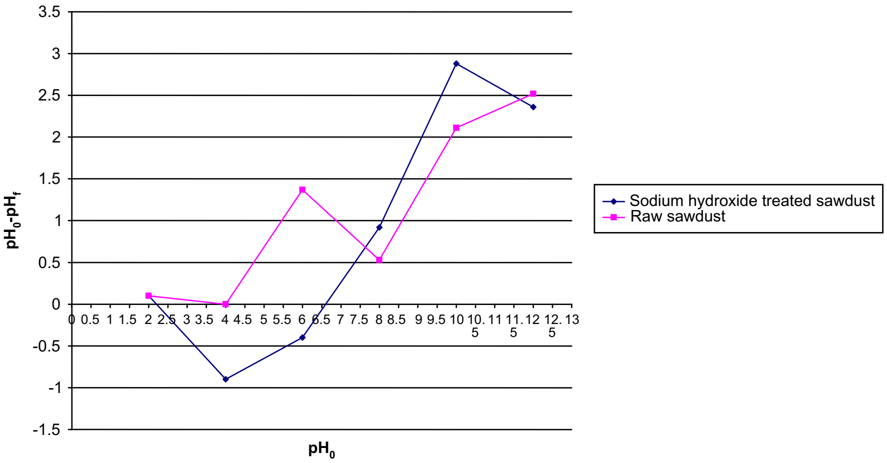

Fig. 8. Plot of pH_0 against (pH_0–pH) for raw and chemically treated *African beech* sawdust.

dust was broadened and shifted to 2918 cm^{-1} after treating the sawdust with NaOH. The peaks at 1631 and 1059 cm^{-1} observed on raw sawdust got split into (1650 and 1560 cm^{-1}) and (1020 and 1040 cm^{-1}) respectively. Also in comparing the FTIR of the adsorbents before and after adsorption, it was observed that there was a shift in the wave numbers of some peaks associated with the metal ions loaded adsorbents.

Table 8 summarizes the main surface functional groups of raw and treated sawdust before and after adsorption of the studied metal ions.

3.5. Scanning electron microscope (SEM) analysis

The surface structures of *African beech* wood sawdust (raw and chemically treated) were analyzed using scanning electron microscope (SEM) as given in (Fig. 10). The microphotographs of both adsorbents revealed clearly the presence of irregular, asymmetric pores, and macroporous structures. According to Rahman and Islam [44], this porous structure might be the reason of high metal ions adsorption due to providing high internal surface area (Fig. 10).

3.6. Thermogravimetric analysis

According to Kalderis et al. [45], thermoanalytical techniques have been widely used to study the thermal behavior of agricultural by-products and therefore, it is possible that thermal analysis would make an important contribution to knowledge of the thermal behavior of biomass.

Our TGA results presented in Fig. 11a reveals three main steps of weight loss occurring at the heating rate of 10℃/min. The first step of weight loss for both adsorbents was observed from the start of the experiment until the temperature of 100℃, the amount of weight loss recorded, was attributed to the loss of moisture present in the sample and the external water bound by surface tension [45]. The second weight loss step occurred between 100 and 400℃ in case of raw sawdust and between 100 and 350℃ for

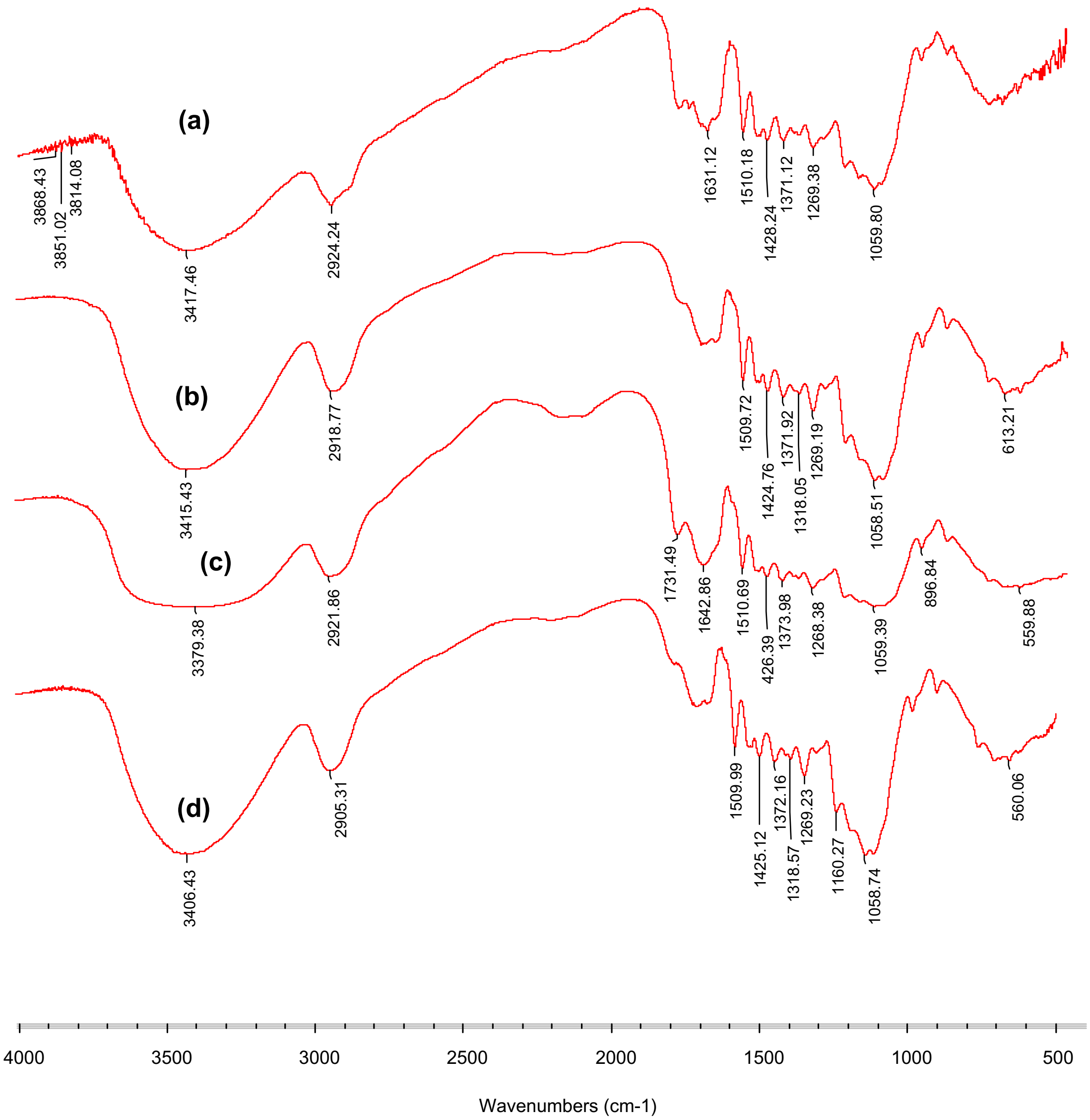

Fig. 9. FTIR spectra of raw and chemically treated *African beech* sawdust (a, b) before and (c, d) after adsorption, respectively.

the chemically treated sawdust. This step was attributed due to the removal of volatile matter which corresponded to the decomposition of the three major sawdust components, cellulose, hemicellulose, and lignin [45]. The third weight loss step observed after 400℃ in case of raw sawdust and above 350℃ for the chemically treated sawdust was assigned to the transformation of cellulose, hemicellulose and lignin intermediates to gaseous materials and tars [45]. The TGA curves also revealed that the maximum rate of weight loss occurred at rapid decomposition of the samples between 200 and 400℃ in case of raw sawdust and between 200 and 350℃ for the chemically treated sawdust.

As can be seen from Fig. 11b, the DTG pattern of raw sawdust exhibited only one prominent wave of weight loss (between 200 and 400℃) with a maximum centered at 393.26℃. Impregnation with sodium hydroxide brought about remarkable modifications in case of the chemically treated sawdust. The DTG pattern of chemically treated sawdust shows a regular small weight loss covers the early stage between ambient and 400℃, with a sharp peak at 320.27℃, followed by another slow higher weight loss with increasing temperature from 400 to 700℃ with a weak peak at 468.17℃.

Our thermogravimetric analysis results are in good agreement with the results previously obtained for

Table 8
Surface functional groups observed on raw and treated *African beech* sawdust before and after adsorption by FTIR spectroscopy

Wave-number range (cm^{-1})	Raw sawdust	Treated sawdust	Raw sawdust after adsorption	Treated sawdust after adsorption	Bonds indicative
3500–3200	3400 (sharp)	3400	3379 (broad)	3406	OH stretching of phenol group of cellulose and lignin
3000–2850	2924 (sharp)	2918 (broad)	2921	2905	C–H methyl and methylene groups, C–H stretching
1750–1680	1750	–	1731	–	C=O carbonyls
1670–1640	1631	1650	1642	1640	Carboxylic groups
1640–1500	1510	1560, 1509	1510	1509	Carboxylic groups
1450–1375	1428	1424	1426	1426	Symmetric bending of CH3
1375–1300	1371	1371	1373	1372	C–O stretching of COOH
1300–1000	1269	1269	1268	1269	$-SO_3$ stretching
1350–1000	1059	1020, 1040	1059	1058	O–H alcohols and aliphatic ethers
1300–1000	900	1100	896	900	C–O stretching of COOH
990–690	690	613	559	560	C–H bending, $-SH_2$, $-PO_4$

many lignucellulosic adsorbents including: maize stalks [46], corncob [47], rice husk [48] and cotton stalks [49].

3.7. Desorption study

According to Gupta and Rastogi [50] the metals sorbed on a biomass can be desorbed by a suitable eluant or desorbing solution, and thus biomass can be used in multiple sorption–desorption cycles. In the present study, four different desorption solutions were used including 0.1 M HCl, HNO_3, and H_2SO_4 and 0.5 M NaOH. Fig. 12 shows the percentages of aluminum, iron, copper, zinc, and lead ions released from raw and treated sawdust after treatment with different desorption solutions. Our results indicated that the tested desorption solutions are capable of recovering the studied metal ions with varying percentages. Whereas the best recovery percentages of iron, copper, and zinc were achieved using 0.1 M (HCl) from both adsorbents; higher recovery of aluminum and lead was obtained using 0.1 M (HNO_3).

4. Conclusion

Adsorbents prepared from *African beech* sawdust were successfully used for simultaneously removing aluminum, iron, copper, zinc, and lead ions from their

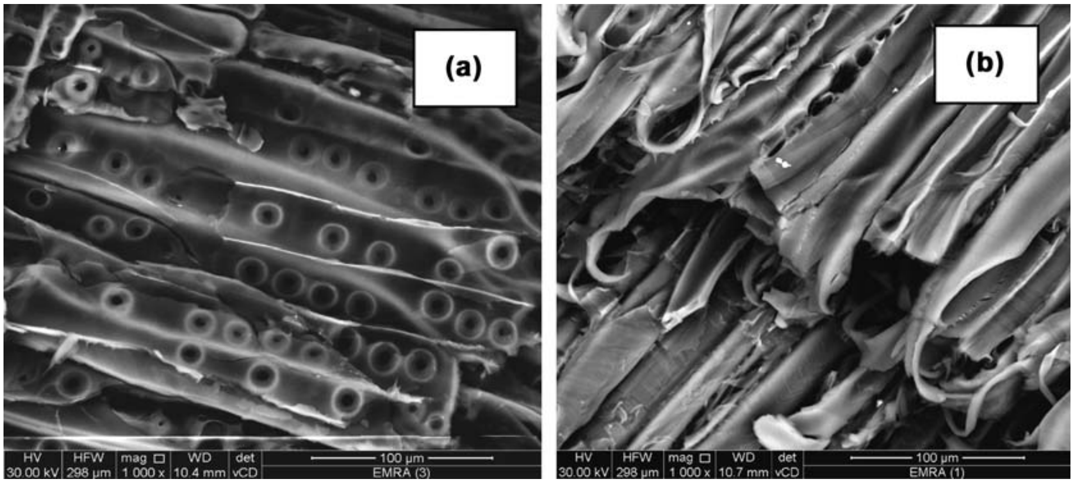

Fig. 10. Scanning electron microscope photos of (a) raw and (b) chemically treated *African beech* sawdust.

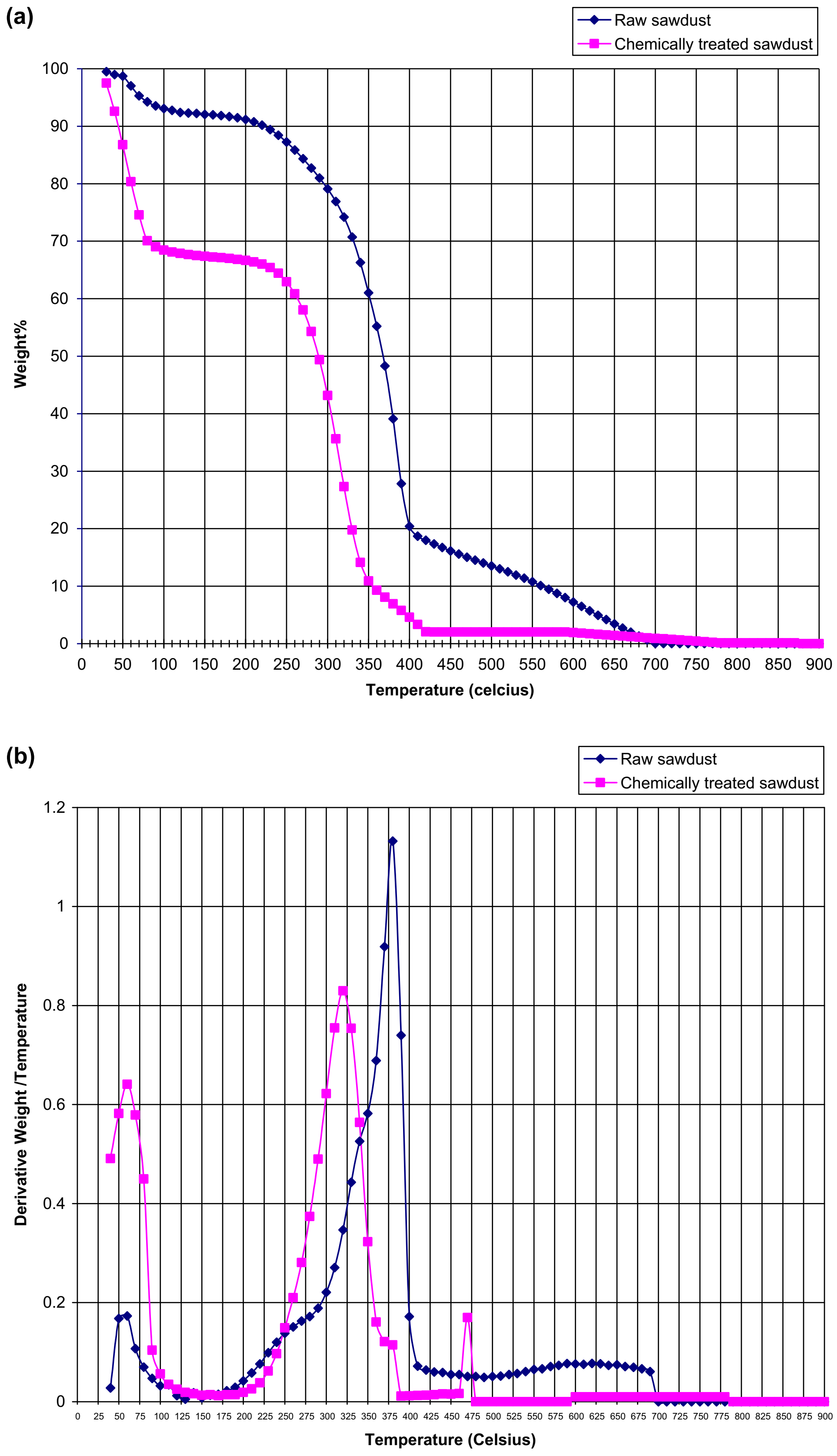

Fig. 11. (a) TGA of raw and chemically treated sawdust and (b) DTG of raw and chemically treated sawdust.

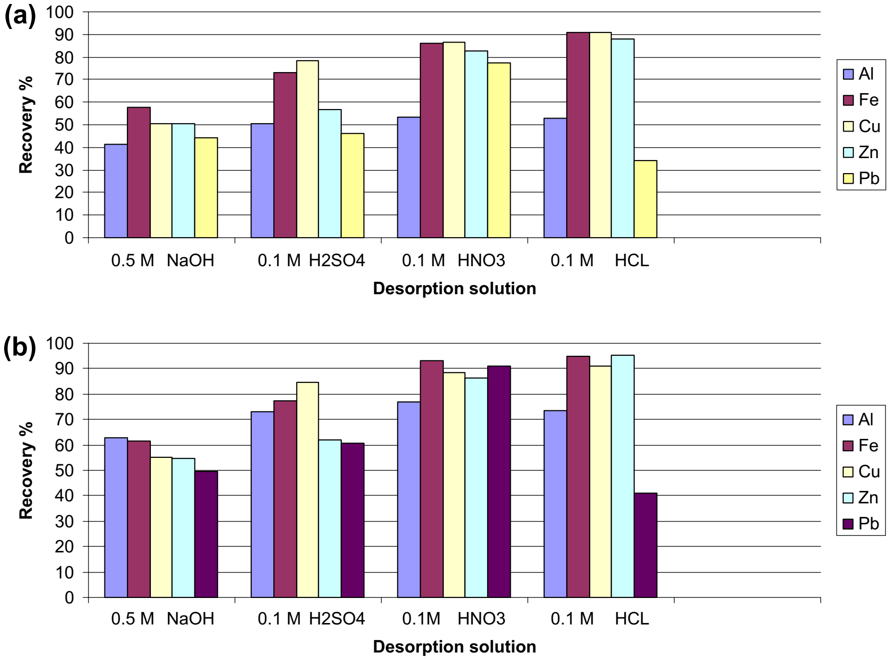

Fig. 12. Metal ions recovery percentages from (a) raw and (b) chemically treated *African beech* sawdust using different desorption solutions.

mixed ions solution. The obtained data revealed that under the same experimental conditions the chemical treatment of sawdust enhanced the removal percentages of the studied metal ions compared to raw sawdust. The metal ions removal onto the studied adsorbents followed the pseudo-second-order kinetic and the Langmuir isotherm models. The recovery of the adsorbed ions was successfully achieved using different desorption solutions. *African beech* sawdust could be used to prepare low-cost adsorbents for the treatment of wastewater contaminated by various metal ions.

References

[1] A. Takaharu, W. Pi-Chao, I. Akio, Spectrophotometric detection of labile zinc(II) released from metallothionein: a simple method to evaluate heavy metal toxicity, J. Biosci. Bioeng. 109 (2009). 638–644. doi: 10.1016/j.jbiosc.2009.11.016.

[2] T. Xiao-Wu, W. Yan, L. Zhen-Ze, Removal of heavy metal from aqueous solutions using chinese loess soil, Adv. Environ. Geotech. 2 (2010) 314–319.

[3] M.H. Nasir, R. Nadeem, K. Akhtar, M.A. Hanif, A.M. Khaild, Efficacy of modified distillation sludge of rose (*Rosa centifolia*) petals for lead(II) and Zn (II) removal from aqueous solutions, J. Hazard. Mater. 147 (2007). 1006–1014. doi: 10.1016/j.jhazmat.2007.01.131.

[4] L. Hu, A.A. Adeyiga, T. Greer, E. Miamee, A. Adeyiga, Removal of metal ions from wastewater with roadside tree leaves, Chem. Eng. Commun. 189 (2002). 1587–1597. doi: 10.1080/00986440214581.

[5] D.Y. Zhang, Y. Ma, Y. Wang, H.X. Feng, J. Chen, J.C. Zhu, Y. Hao, Preparation and characterisation of sulfonic acid-functionalized carbon/loess, Adv. Mater. Res. 194–196 (2011). 1652–1655. doi: 10.4028/www.scientific.net/AMR.194-196.1652.

[6] J.R. Deans, B.G. Dixon, Uptake of Pb^{2+} and Cu^{2+} by novel biopolymers, Water Res. 26 (1992). 469–472. doi: 10.1016/0043-1354(92)90047-8.

[7] N.A.A. Babarinde, J. Oyebamiji Babalola, R. Adebowale Sanni, Biosorption of lead ions from aqueous solution by maize leaf, Int. J. Phy. Sci. 1 (2006) 23–26.

[8] F. Pagnanelli, S. Mainelli, F. Veglio, I. Michelis, D.F. Beolchini, L. Toro, Olive pomace for heavy metal removal: Adsorbent characterisation and equilibrium modelling, Acta. Metall., Slovaca 12 (2006). 313–320. doi: 10.1016/j.ces.2003.08.001.

[9] S. Gueu, B. Yao, K. Adouby, G. Ado, Kinetics and thermodynamics study of lead adsorption on to activated carbons from coconut and seed hulls of the palm tree, Int. J. Environ. Sci. Technol. 4 (2007) 11–17.

[10] N.T. Abdel-Ghani, M. Hefny, G.A.F. El-Chaghaby, Removal of lead from aqueous solution using low cost abundantly available adsorbents, Int. J. Environ. Sci. Technol. 4 (2007) 67–73.

[11] N.T. Abdel-Ghani, A.K. Hegazy, G.A. El-Chaghaby, Typha domingensis leaf powder for decontamination of aluminum, iron, zinc and lead: adsorption kinetics and equilibrium modeling, Int. J. Environ. Sci. Technol. 6 (2009) 243–248.

[12] A.J. Al-Ithari, A. Sathasivan, R. Ahmed, H.B. Vuthaluru, W. Zhana, M. Ahmed, Superiority of date seed ash as an adsorbent over other ashes and ferric chloride in removing boron from seawater, Desal. Wat. Treat. 32 (2011). 324–328. doi: 10.5004/dwt.2011.2717.

[13] L.H. Huang, Y.Y. Sun, Q.K. Yue, Q. Yue, L. Li, B. Gao, Adsorption of Cd (II) on lotus stalks-derived activated carbon: batch and column studies, Water Treat. 41 (2012). 122–130. doi: 10.1080/19443994.2012.664697.

[14] A.G.S. Prado, A.O. Moura, R.D.A. Andrade, I.C. Pescara, V.S. Ferreira, E.A. Faria, A.H.A. Oliveira, E.Y.A. Okino, L.F. Zara, Application of Brazilian sawdust samples for chromium removal from tannery wastewater, J. Therm. Anal. Calorim. 99 (2010). 681–687. doi: 10.1007/s10973-009-0284-0.

[15] M.H. Kalavathy, R.M. Lima, Comparison of copper adsorption from aqueous solution using modified and unmodified *Hevea brasiliensis* sawdust, Desalination 255 (2010). 165–174. doi: 10.1016/j.desal.2009.12.028.

[16] S. Lagergren, Zur theorie der sogenannten adsorption gelöster stoffe, Kungliga Svenska, Vetenskapsakademiens Handlingar, Band 24(41–39) (1898).

[17] Y.S. Ho, G. Mckay, Application of kinetic models to the sorption of copper (II) onto peat, Adsorpt. Sci. Technol. 20 (2002). 797–815. doi: 10.1260/026361702321104282.

[18] W.J. Weber, Jr., J.C. Morris, Kinetics of adsorption on carbon from solution, J. Sanit. Eng. Div. Am. Soc. Civ. Eng. 89 (1963) 31–60.

[19] I. Langmuir, The adsorption of gases on plane surfaces of glass, mica and platinum, J. Am. Chem. Soc. 40 (1918) 1361–1368.

[20] H.M.F. Freundlich, "über die adsorption" in lösungen, Z. Phys. Chem. 57 (1906) 385–470.

[21] K.W. Kolasniski, Surface Science, Wiley, Chister, 2001.

[22] M. Rafatullah, O. Sulaiman, R. Hashim, A. Ahmad, Adsorption of copper (II), chromium (III), nickel (II) and lead (II) ions from aqueous solutions by *meranti sawdust*, J. Hazard. Mater. 170 (2009). 969–977. doi: 10.1016/j.jhazmat.2009.05.066.

[23] M. Sciban, M. Klasnja, B. Skrbic, Modified softwood sawdust as adsorbent of heavy metal ions from water, J. Hazard. Mater. B136 (2005). 266–271. doi: 10.1016/j.jhazmat.2005.12.009.

[24] H. Rehman, M. Shakirullah, I. Ahmad, S. Shah, Hameedullah Sorption studies of nickel ions onto sawdust of *Dalbergia sissoo*, J. Chin. Chem. Soc. 53 (2006) 1045–1052.

[25] T. Robinson, B. Chandran, P. Nigam, Effect of pretreatments of three waste resiudes, wheat straw, corncobs and barley husks on dye adsorption, Bioresour. Technol. 85 (2002) 119–124.

[26] S. Benyoucef, M. Amrani, Removal of phosphorus from aqueous solutions using chemically modified sawdust of Aleppo pine (*Pinus halepensis Miller*): kinetics and isotherm studies, Environmentalist 31 (2011). 200–207. doi: 10.1007/s10669-011-9313-1.

[27] P. Chingombe, B. Saha, R.J. Wakeman, Sorption of atrazine on conventional and surface modified activated carbons, J. Colloid Interface Sci. 302 (2006) 408–416. http://dx.doi.org/10.1016/j.jcis.2006.06.065.

[28] H.K. Boparai, M. Joseph, D.M. O'Carroll, Kinetics and thermodynamics of cadmium ion removal by adsorption onto nano zerovalent iron particles, J. Hazard. Mater. 186 (2011) 458–465. http://dx.doi.org/10.1016/j.jhazmat.2010.11.029.

[29] C. Theivarasu, S. Mylsamy, Equilibrium and kinetic adsorption studies of Rhodamine-B from aqueous solutions using cocoa (*Theobroma cacao*) shell as a new adsorbent, Int. J. Eng. Sci. Technol. 2 (2010) 6284–6292.

[30] D. Kavitha, C. Namasivayam, Experimental and kinetic studies on methylene blue adsorption by coir pith carbon, Bioresour. Technol. 98 (2007) 14–21. http://dx.doi.org/10.1016/j.biortech.2005.12.008.

[31] G.S. Gupta, G. Prasad, K.K. Panday, V.N. Singh, Removal of chrome dye from aqueous solutions by fly ash, Water Air Soil Pollut. 37 (1987). 13–24. doi: 10.1007/BF00226476.

[32] M. Ozacar, Equilibrium and kinetic modeling of adsorption of phosphorus on calcined alunite, Adsorption 9 (2003) 125–132.

[33] M. Ghaed, B. Sadeghian, A. Amiri Pebdani, R. Sahraei, A. Daneshfar, C. Duran, Kinetics, thermodynamics and equilibrium evaluation of direct yellow 12 removal by adsorption onto silver nanoparticles loaded activated carbon, Chem. Eng. J. 187 (2012) 133–141. http://dx.doi.org/10.1016/j.cej.2012.01.11.

[34] Z. Baysal, E. Çinar, Y. Bulut, H. Alkan, M. Dogru, Equilibrium and thermodynamic studies on biosorption of Pb(II) onto *Candida albicans* biomass, J. Hazard. Mater. 161 (2009) 62–67. http://dx.doi.org/10.1016/j.jhazmat.2008.02.122.

[35] D.B. Singh, G. Prasad, D.C. Rupainwar, V.N. Singh, As (III) removal from aqueous solution by adsorption, Water Air Soil Pollut. 42 (1988). 373–386. doi: 10.1007/BF00279281.

[36] A.A. Zaid, A.M. Mohammed, Batch adsorption of cadmium ions from aqueous solution by means of olive cake, J. Hazard. Mater. 151 (2008). 194–201. doi: 10.1016/j.jhazmat.2007.05.069.

[37] M.E. Argun, S. Dursun, C. Ozdemir, M. Karatas, Heavy metal adsorption by modified oak sawdust: thermodynamics and kinetics, J. Hazard. Mater. 141 (2007). 77–85. doi: 10.1016/j.jhazmat.2006.06.095.

[38] D. Bőzić, V. Stanković, M. Gorgievski, G. Bogdanović, R. Kovačević, Adsorption of heavy metal ions by sawdust of deciduous trees, J. Hazard. Mater. 171 (2009). 684–692. doi: 10.1016/j.jhazmat.2009.06.055.

[39] B. Yu, Y. Zhang, A. Shukla, S.S. Shukla, K.L. Dorris, The removal of heavy metals from aqueous solutions by sawdust adsorption-removal of lead and comparison of its adsorption with copper, J. Hazard. Mater. B84 (2001). 83–85. doi: 10.1016/S0304-3894(01)00198-4.

[40] M.S. Onyango, Y. Kojima, O. Aoyi, E.C. Bernardo, H. Matsuda, Adsorption equilibrium modeling and solution chemistry dependence of fluoride removal from water by trivalent-cation-exchanged zeolite F-9, J. Colloid Interface Sci. 279 (2004). 341–350. doi: 10.1016/j.jcis.2004.06.038.

[41] N.Z. Muhammad, N. Raziya, A.H. Muhammad, Biosorption of nickel from protonated rice bran, J. Hazard. Mater. 143 (2007). 478–485. doi: 10.1016/j.jhazmat.2006.09.055.

[42] F. Gode, E.D. Atalay, E. Pehlivan, Removal of Cr(VI) from aqueous solutions using modified red pine sawdust, J. Hazard. Mater. 152 (2008). 1201–1207. doi: 10.1016/j.jhazmat.2007.07.104.

[43] M.A. Wahab, S. Jellali, N. Jedidi, Ammonium biosorption onto sawdust: FTIR analysis, kinetics and adsorption isotherms modeling, Bioresour. Technol. 101 (2010). 5070–5075. doi: 10.1016/j.biortech.2010.01.121.

[44] M.S. Rahman, M.R. Islam, Effects of pH on isotherms modeling for Cu(II) ions adsorption using maple wood sawdust, Chem. Eng. J. 149 (2009). 273–280. doi: 10.1016/j.cej.2008.11.029.

[45] D. Kalderis, S. Bethanis, P. Paraskeva, E. Diamadopoulos, Production of activated carbon from bagasse and rice husk by a single-stage chemical activation method at low retention times, Bioresour. Technol. 99 (2008). 6809–6816. doi: 10.1016/j.biortech.2008.01.041.

[46] A.A. El-Hendawy, Surface and adsorptive properties of carbons prepared from biomass, Appl. Surf. Sci. 252(2) 287–295. doi:10.1016/j.apsusc.2004.11.092.

[47] Y. Sun, P.A. Webley, Preparation of activated carbons from corncob with large specific surface area by a variety of chemical activators and their application in gas storage, Chem. Eng. J. 162 (2010) 883–892. http://dx.doi.org/10.1016/j.cej.2010.06.031.

[48] T. Liou, S. Wu, Characteristics of microporous/mesoporous carbons prepared from rice husk under base- and acid-treated conditions, J. Hazard. Mater. 171 (2009) 693–703.

[49] M.A. Nahil, P.T. Williams, Pore characteristics of activated carbons from the phosphoric acid chemical activation of cotton stalks, Biomass Bioenergy 37 (2012) 142–148.

[50] V.K. Gupta, A. Rastogi, Sorption and desorption studies of chromium (VI) from nonviable cyanobacterium *Nostoc muscorum* biomass, J. Hazard. Mater. 154 (2008). 347–354. doi: 10.1016/j.jhazmat.2007.10.032.